

REVIEW

Which Design Constraints Apply to a Pipe-Framed Greenhouse?: From Perspectives of Structural Engineering, Meteorological Conditions, and Wind Engineering

Hideki MORIYAMA^{1*}, Sadanori SASE², Limi OKUSHIMA¹ and Masahisa ISHII¹

¹ Agricultural Environment Engineering Research Division, National Institute for Rural Engineering, NARO (Tsukuba, Ibaraki 305-8609, Japan)

² College of Bioresource Sciences, Nihon University (Fujisawa, Kanagawa 252-0880, Japan)

Abstract

Many studies related to greenhouse design have been conducted. This paper reviewed five results of research into the design of pipe-framed greenhouses (hereinafter pipe houses) using an investigation, numerical analysis and wind-tunnel test. The first and second studies showed how the pipe houses collapsed due to snow and wind load. The third study analyzed an economical and reasonable design for a typical pipe house subject to snow load. Seven numerical finite element models of simple pipe house were subject to stress and buckling analyses. In the fourth study, the distributions of wind pressure coefficient C_p , both external and internal, were evaluated in detail using a pipe-house model, based on a wind-tunnel experiment using 1:20 scale models in a turbulent boundary layer correctly simulating natural winds over typical open-country exposure. The fifth study investigated the effect of d_p , the distance between the side walls of pipe houses, on the distribution of C_p on two or three pipe houses arranged in parallel. The results of these studies are indispensable to establish safe and economical pipe-house designs.

Discipline: Agricultural engineering

Additional key words: high tunnel, numerical analysis, snow load, wind pressure coefficient, wind-tunnel test

Introduction

Globally, plastic film-clad greenhouses are widely used in agricultural and horticultural industries. Such greenhouses are usually designed to a lower level of structural safety than conventional building structures, because of the need to minimize initial costs, the demand for higher light transmission, reduced injury risk and so on.

Pipe-framed greenhouses (hereinafter pipe houses), which include high tunnels, are simpler structures. A pipe house mainly comprises lightweight arch- and straight pipes covered with plastic film, which farmers can easily construct single-handed. Given the relatively high cost of labor in Japan, having farmers construct such pipe houses themselves is helpful to decrease the overall greenhouse construction cost. In fact, pipe houses comprise approximately

80 % of the total area of greenhouses in Japan and hence play an important role in agricultural and horticultural industries there. However, it is also a fact that most of the wind and snow damage inflicted on greenhouses affects pipe houses. Okushima & Nara (1992) used statistical tables concerning damage to greenhouses to determine that the extent of damage to greenhouses caused by snow and wind load as a proportion of overall damage was about 80 %. Wind and snow loads are the key external forces that determine pipe-house design.

However, little research has been conducted into the resistance of standard pipe greenhouses to snow load in Japan. Ogawa et al. (1989) indicated that one important factor to consider in a theoretical analysis was the support condition at the soil. If the arch pipe is inserted in firm, unsaturated ground the analytical value determined by a numerical model of the pipe house with fixed support at the

*Corresponding author: e-mail hmori@affrc.go.jp

Received 11 November 2013; accepted 8 May 2014.

ground connection can be used for the analysis and compared with an experimental value. Yamashita & Osari (1980) determined the optimum section shape for snow load and wind pressure by numerical analysis. However, these section shapes were only evaluated based on the criterion of improving mechanical strength. There was no consideration of the ease of use for practical construction by a farmer working alone.

In terms of wind load, wind-tunnel tests and numerical analyses were performed to determine the recommended design wind pressure for greenhouses. Sase et al. (1980) conducted experiments in wind-tunnel tests considering the vertical distribution of the wind, and determined the distribution of wind pressure on the single-span gable greenhouse. Hoxey & Richardson (1984) also measured the surface pressure of full-scale pipe houses under natural wind conditions, while Mathews & Meyer (1987), and Mistriotis & Briassoulis (2002) calculated wind pressure coefficients for the semicircular greenhouse numerically. Robertson et al. (2002) determined the wind pressure coefficients of semicircular and flat-roof greenhouses covered with plastic film and net by wind-tunnel tests. Although several investigations have been conducted into wind loads on greenhouses, no study has been made on the pipe houses which are popular in Japan. A cross-section of the pipe house reveals slanted walls, curvature at the eaves and a pointed arch. The shape is more complicated than those in previous studies, which results in a different pressure distribution.

Investigation into damaged pipe houses

Moriyama et al. (1999) summarized the results of the field study of pipe houses damaged by heavy snow to determine the cause of failure. Important results were determined by a field survey of pipe houses damaged by heavy snow in 1998. For pipe houses under heavy snow, the roof was pushed down and collapsed in a shape resembling the character “M”. Since the arch pipes commonly used in pipe houses have a large slenderness ratio, they are prone to failure by buckling. Accordingly, pipe-house roofs should be reinforced by bracing.

Several arch pipes showed horizontal displacement at ground level. When the support condition is assumed to be fixed, the maximum allowable snow load would be very large. However, in practical applications, the soil is often saturated and softened, and the end condition is mechanically equivalent to a hinged end. The hinged-end condition should also be applied as a support condition for safe design when the pipe house is analyzed.

Investigations of pipe houses damaged by Typhoon 0221 (Moriyama et al. 2003b) often show a collapse where the windward eaves were pushed down by strong winds (Fig. 1). However, when there were side-gable openings



Fig. 1. Collapse of a pipe house caused by strong typhoon winds (Moriyama et al., 2003)

pipe houses, the type of collapse was quite different, whereby the roof was pushed down and collapsed downward. This showed the internal wind pressure was greatly changed by the side-gable openings. Most pipe houses with side-gable openings and doors that could be open tend to fail due to wind pressure. Consequently, the wind pressure coefficient C_p considering side-gable openings should be determined.

Reinforcement for pipe houses subject to snow load

To investigate the effect of adding braces to the pipe house for snow load, Moriyama et al. (2008b) analyzed and compared two types of pipe-house structure. One was the unmodified common pipe house, while another was the same pipe house, but reinforced by one or two steel wires as braces. Numerical calculations were introduced to determine the optimum design for the pipe house subject to snow load. An analytical model of the pipe house for finite element method (FEM) analysis is shown in Fig. 2. The pipe house was 6000 mm width and the ridge height was 3160 mm. This cross-sectional pipe-house design is one of the most popular in Japan. The pipe house comprises two arch pipes with an outside diameter of 25.4 mm and 1.2 mm thick. The arch pipe spacing was assumed to be 50 cm. To determine the influence of the width and ridge height of the pipe house and the section modulus of the arch pipe on the maximum allowable snow load of the pipe house, seven numerical models were analyzed by both stress and buckling analyses (Table 1). Besides, Moriyama et al. (2003a) confirmed that the result of numerical analysis of the pipe-house model subject to snow load effectively matched that from a loading test for full-size pipe houses. There was also a good linear relationship between the maximum allowable

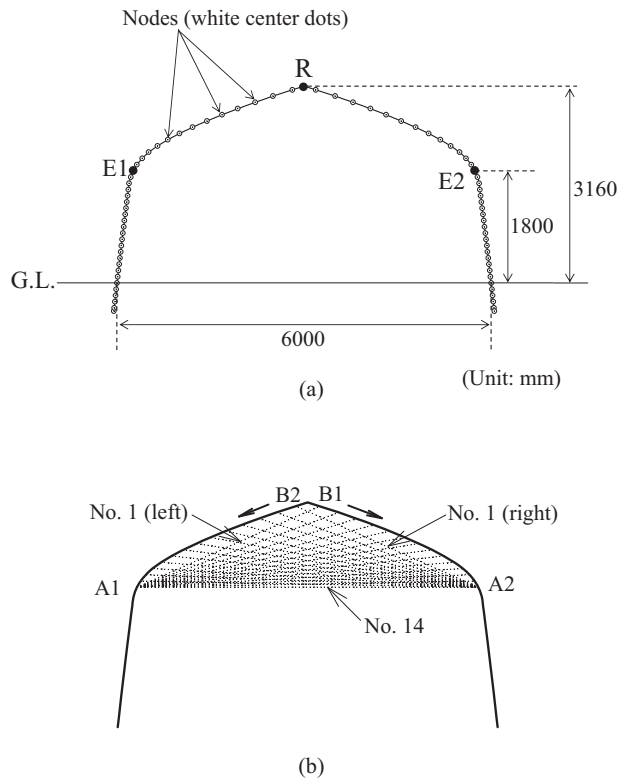


Fig. 2. A numerical model of the pipe house, standard section, for the FEM analysis (Moriyama et al., 2008b)

(a) White center dots represent the nodes of the model; the uniformly distributed load on the roof of the pipe house over the entire span is represented from black dots E1 to E2; the uniformly distributed load on only one side roof is from black dots E1 to R

(b) All pairs of braces from Nos. 1 to 14; height of the upper end of braces, B1 to B2, was lowered from 310 to 180 cm at intervals of 10 cm. The height of the other ends, A1 to A2, remained constant with increasing case No.

snow loads from numerical analyses and those from loading tests.

The width and ridge height of the structure influences the maximum allowable snow load of pipe houses. In stress analysis, the maximum allowable snow load of the pipe house declined with increasing width. For the analytic model without bracing, the maximum allowable snow load of the model 4500 mm width was roughly 300 N/m², which is one of the standard snow loads of the Standard for Structures of Greenhouses, Japan (Japan Greenhouse Horticulture Association 1999). Only narrow pipe houses should be allowed to be constructed on ground softened due to saturation. However, adding braces in the form of a steel wire of diameter 3.2 mm to the roof of the pipe house significantly increased the maximum allowable snow load of the pipe house. Similar results were determined by buckling analysis. Table 2 shows the allowable snow load of unmod-

Table 1. Numerical models for FEM analysis (Moriyama et al., 2008b)

Width (mm)	Ridge height (mm)	Section outline*
4500	2370	
4500	3160	
6000	2370	
6000	3160	
6000	4213	
8000	3160	
8000	4213	

*Shaded is the standard section.

ified and modified standard sections with braces, from Nos. 1 to 14. Italic figures represent the minimum of four allowable snow loads for each of the braced models. In this table, the allowable snow load of the unmodified pipe house was 156 N/m² determined by stress analysis, while the value of 471 N/m² with bracing No. 10 was the largest of fifteen minimum allowable snow load determinations. Consequently, the maximum allowable snow load increased from 156 to 471 N/m² with suitable bracing. However, the maximum allowable snow load of the analytic model 8000 mm width was almost equivalent to the standard snow load. Therefore, the maximum width is 8000 mm if arch pipes of 25.4 mm diameter and 1.2 mm thick are used.

The influence of the ridge height on the maximum allowable snow load differed between stress and buckling analyses. In stress analysis, the ridge height had little influence on the maximum allowable snow load. The maximum allowable snow loads for all analytic models of different ridge heights were roughly half the standard snow load 300 N/m², hence the need to reinforce by adding braces was needed. In buckling analysis, the maximum allowable snow load declined with increasing ridge height and the slenderness ratio of the arch pipe increased. The maximum allowable snow load in buckling analysis was also increased by adding braces. The maximum allowable snow load for the analytic model of 4213 mm ridge height was almost equivalent to the standard snow load. Consequently the highest ridge height was 4213 mm for the safe design of pipe houses.

Table 3 shows the weight of steel mass in the arch pipes and the shading rate of numerical models for each kind of arch pipe. Numerical models were the standard and similar sections. The maximum allowable snow loads were set to 300 N/m² by adjusting pipe spacing to ensure that the widest spacing according to the design criterion was used in each case. The steel mass and shading rate of pipe houses with larger and wider-spaced pipes were less than those of

Table 2. The allowable snow load obtained by stress and buckling analyses for every bracing patterns in a pipe house 6000 mm width, with ridge height of 3160 mm, and arch-pipe diameter of 25.4 mm (Moriyama et al., 2008b)

Bracing	Allowable snow load by stress analysis (N/m ²)		Allowable snow load by buckling analysis (N/m ²)	
	Load on entire span	Load on one side roof	Load on entire span	Load on one side roof
none	156	246	247	487
No.1	151	243	396	753
No.2	255	358	372	733
No.3	236	423	377	749
No.4	268	463	387	769
No.5	309	494	399	792
No.6	351	538	413	819
No.7	392	633	428	501
No.8	434	612	443	490
No.9	477	601	458	481
No.10	521	537	471	474
No.11	569	485	480	469
No.12	621	443	476	467
No.13	677	408	410	469
No.14	745	378	237	473

Table 3. The steel mass and shading rate of the standard-section insulation and a similar unmodified common pipe house obtained by stress analysis (Moriyama et al., 2008b)

Arch pipe		Width (mm)	Ridge height (mm)	Pipe spacing (cm)	Steel mass (kg/m ²)	Shading rate (%)
Diameter (mm)	Thickness (mm)					
19.1	1.1	8000	4213	6	14.60	31.8
		6000	3160	13	6.74	14.7
		4500	2370	24	3.65	8.0
25.4	1.2	8000	4213	13	9.89	19.5
		6000	3160	26	4.95	9.8
		4500	2370	48	2.68	5.3
31.8	1.6	8000	4213	29	7.37	11.0
		6000	3160	55	3.89	5.8
		4500	2370	101	2.12	3.1
38.1	1.8	8000	4213	49	5.90	7.8
		6000	3160	90	3.21	4.2
		4500	2370	163	1.77	2.3
42.7	2.0	8000	4213	69	5.23	6.2
		6000	3160	127	2.84	3.4
		4500	2370	228	1.58	1.9

Support conditions were all hinged end.
Load was on the entire span.

pipe houses with smaller and more closely spaced pipes. For example, the steel mass and shading rate of the standard section, including the arch pipe of 19.1 mm diameter were 6.74 kg/m² and 14.7 %. Conversely, for the pipe house constructed by the arch pipe of 42.7 mm diameter, the steel mass and shading rate were 2.84 kg/m² and 3.4 %. Moreover, the difference in steel mass and shading rate

caused by the size of pipe houses declined with increasing section modulus of the arch pipe. These results were calculated by stress analysis and the trend of results determined by buckling analysis was almost equivalent to the result determined by stress analysis. The pipe spacing was 6 to 24 cm for the arch pipe of 19.1 mm diameter. Pipe spacing of pipe houses constructed in the field is much wider, generally

equating to 50 cm or more. For the un-braced standard pipe-house design, an arch pipe of at least 31.8 mm in diameter and 1.6 mm thick should be used.

Most importantly, adding two simple wire braces significantly increased the maximum allowable snow load for all structural sizes and shapes. For structures modified by adding two tension braces at points between 63 to 70 % of the ridge height, the allowable snow load was increased. With braces, the arch spacing can also be increased, thereby reducing the mass of steel needed and reducing shading.

Wind pressure coefficient of a pipe house

One key cause of pipe-house wind disasters may be a lack of knowledge of wind-resistance performance and wind loads on such structures, hence the need to improve the design wind resistance for pipe houses. In particular, the wind pressure coefficients C_p to be used when designing pipe houses should be adequately estimated. To obtain the precise C_p distribution of pipe houses, the pressure exerted on the surface of pipe-house models was measured using a wind tunnel (Moriyama et al. 2008a). All experiments were carried out in an Eiffel-type wind tunnel at the National Institute for Rural Engineering, which has a test section 20 m long, 4 m wide, and 3 m high (Fig. 3). The C_p distributions on a pipe house were also evaluated with a 1:20 scale model in a turbulent boundary layer. A pipe house with the following dimensions was chosen as the subject of the former study as one of the most typical constructed in Japan; 50 m long, 6 m wide, ridge height of 3.16 m, and eaves height of about 1.75 m (Fig. 4). The ratio of length per width was 8.3, sufficient to achieve a virtually two-dimensional flow in the middle part of the model for a wind normal to the ridge. The values of C_p , both external and internal, were defined as follows:

$$C_p = \frac{P - P_s}{\frac{1}{2} \rho U_H^2} \quad (1)$$

where P is the pressure acting on the model (Pa); P_s is the static pressure in the wind tunnel (Pa); ρ is the air density (kg/m^3); and U_H is the wind velocity at the ridge height (m/s). The wind direction $\theta = 0^\circ$ represents the wind direction normal to the ridgeline. θ varied from 0 to 90° at increments of 5° .

Based on the test result, at the central cross-section, the C_p value of the pipe house was 0.45 at the mid-height of the windward wall. The C_p value on the windward roof was negative, gradually increasing in magnitude from 0 at the windward edge to -0.6 at the ridge. On the leeward roof and wall, the values of C_p were -0.6 and -0.54, respectively.

The wind-force coefficient C_f distribution of the pipe house, which is defined as the difference between the external and internal pressure coefficients C_{pe} and C_{pi} , differed

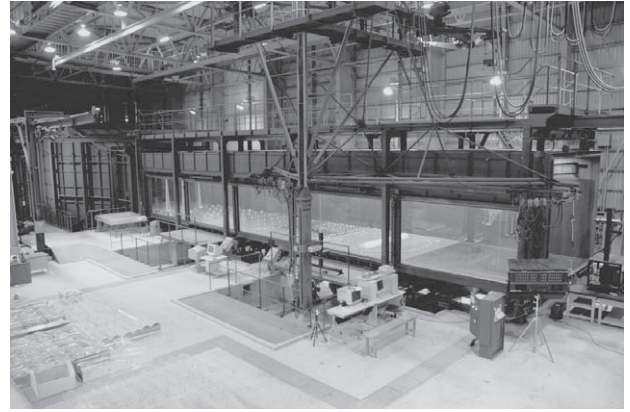


Fig. 3. The Eiffel-type wind tunnel at the National Institute for Rural Engineering

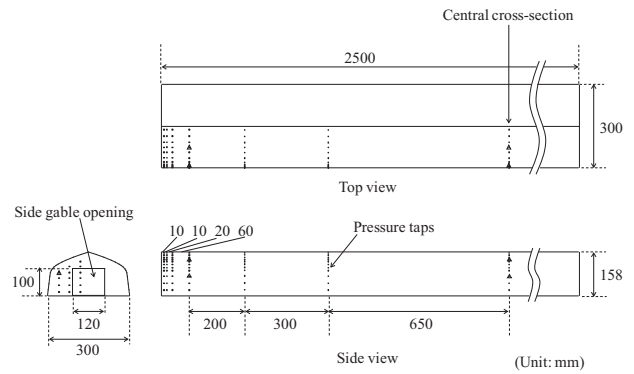


Fig. 4. Scale model used in the wind tunnel experiment; black dots represent the location of the pressure taps; triangles represent the location of the inside pressure taps (Moriyama et al., 2008a)

from that of the specification for a greenhouse with a circular-arc roof (Fig. 5). The distribution resembled that for the gable-roofed greenhouse. However, the C_f value on the windward roof for the pipe house was larger in magnitude than that of the gable-roofed greenhouse.

The C_p distributions of the cross-section in the middle part of the pipe house were independent of the distance from the gable wall. For the part closer to the gable walls, the further away the cross-section from the gable wall, the more significant the difference in C_p distribution for the pipe house became; particularly on the leeward roof and wall. This feature was related to a three-dimensional effect of the flow due to the gable walls. It emerged that a wind-tunnel model with length 4 or more times longer than its width should be used when $\theta = 0^\circ$.

The magnitude of the largest negative C_p value increased and the area of larger suction expanded along the ridgeline with increasing wind direction. When $\theta = 25^\circ$, the maximum negative C_p value was -3.46 at a point near the gable wall (Fig. 6). Conversely, the C_p distribution at the

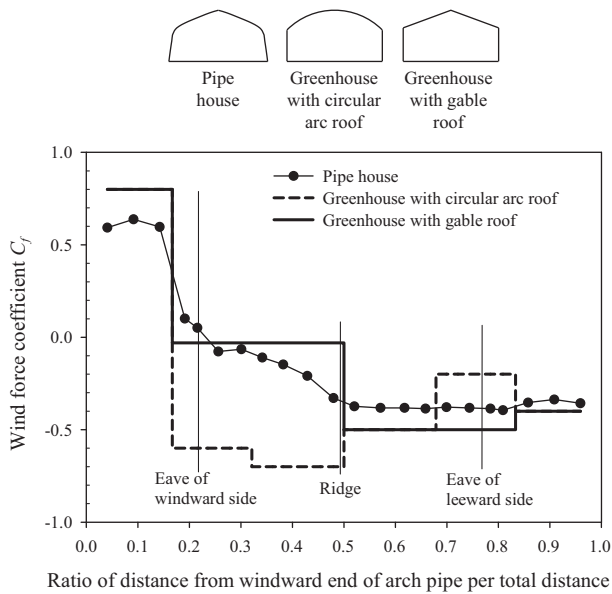


Fig. 5. C_f at the central cross-section of the enclosed model for a wind normal to the ridgeline ($\theta = 0^\circ$) (Moriyama et al., 2008a)

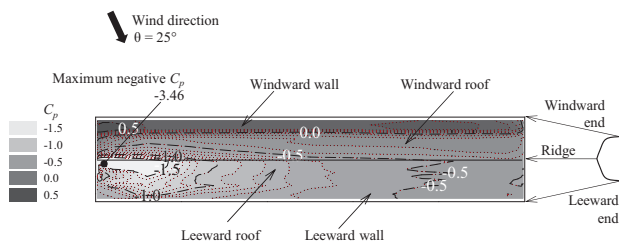


Fig. 6. Distribution of C_p ($\theta = 25^\circ$); the maximum negative value -3.46 occurred at a point near the gable wall (Moriyama et al., 2008a)

central cross-section was not significantly affected by the gable wall within the range 0 to 35° in θ .

The C_{pe} distribution was unaffected by the existence of openings on the gable wall. Conversely, for the pipe house with openings on one or both gable walls, the average C_{pi} values were approximately -0.9 when $\theta = 0^\circ$. This value was much larger in magnitude than the current standard of -0.2 for enclosed greenhouses. With this value, the resultant C_f was as large as 1.35 on the windward wall, and may cause pipe houses with openings designed for the lower standard to collapse.

For pipe houses with openings on windward gable walls, when $\theta = 90^\circ$, the C_{pi} value was 0.46, while a large C_{pe} value of approximately -0.9 emerged in the area close to the windward gable wall, particularly on the roof. High suction combined with C_{pi} and C_{pes} , may result in large uplift forces on the frames near the windward edge. This feature is important when designing foundations.

Single-span pipe houses arranged in parallel

It is common for several single-span pipe houses to be arranged in parallel. Here, the C_p distributions on the pipe houses may be affected by adjacent pipe houses, particularly when the wind direction is perpendicular to the ridgeline. Because the leeward pipe house is placed in the wake of the windward pipe house, the C_p distribution on the leeward pipe house may change significantly. The distance d_p between the side walls of pipe houses plays an important role on the C_p distribution. In practice, the distance d_p is determined by the light requirements for plants grown inside the pipe houses as well as on land constraints. If the C_p distribution on each pipe house for various arrangements has been determined in detail, each pipe house can be reinforced or designed appropriately to achieve the required wind resistance. Moriyama et al. (2010) determined the C_p distributions of windward and leeward models for two pipe houses constructed near each other, and the C_p distributions of windward, leeward and middle models between windward and leeward models for three pipe houses constructed using a wind tunnel. The distance d_p between pipe houses was defined as the gap between the sidewalls of two models, as shown in Fig. 7. Although the actual value of d_p in the field ranges from 1 to several meters, the d_p value varied from 0.25H to 6H (0.79 to 18.96 m in full scale) in this study. The ridge height H was used as the reference length of the model.

Fig. 8 shows that the shape of the C_p distribution on the windward model resembled that of the isolated model (standard C_p distribution), while the C_p values on the roof and leeward wall were negative and dependent on d_p . For realistic values of d_p , e.g. $d_p < 5$ m, the C_p value increased from approximately -0.8 for $d_p = 0.25H$ to approximately -0.6 for $d_p = 1.5H$, which was almost equivalent to that of the standard C_p distribution. Fig. 9 showed the C_p distribution at the central cross-section of the leeward model in the two-model case. The distribution was quite different from the standard C_p distribution, represented by the solid line. The C_p values on the middle and leeward models were negative over the whole area for the range of d_p tested in the present article ($d_p = 0.25H$ to 6H). The influence of d_p on the C_p distribution was significant on the windward wall of the second model. High suctions ($C_p = -0.7$ to -1.0) were induced on the leeward roof near the ridge of the leeward model in the two-model case. Fig. 10 shows the sketch of the flow pattern of separation and re-attachment on the surface of two pipe houses. The flow separated at the ridge of the windward model (point A) and the separated flow passed over the leeward model in most cases. However, the flow was highly unsteady, and the separated flow instantaneously reattached at point B on the windward roof of the leeward model. The reattached flow separated again at the ridge of

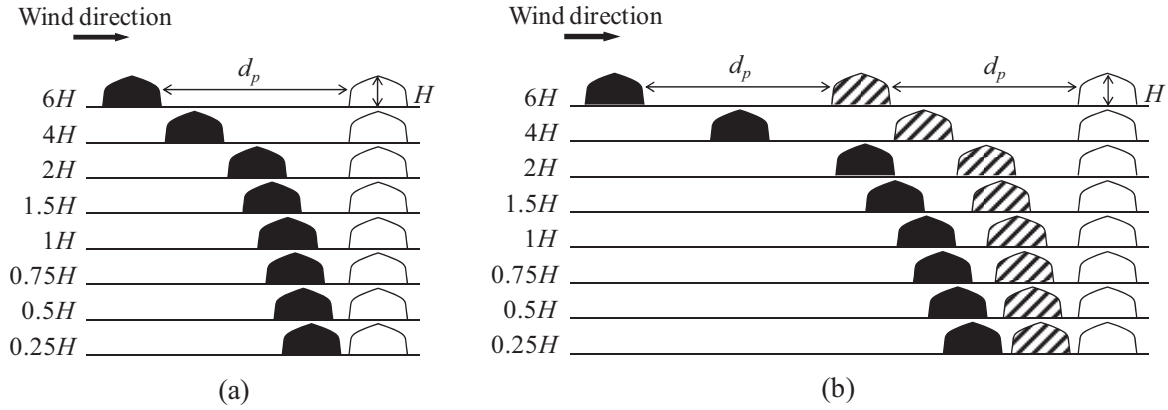


Fig. 7. Distance between pipe houses tested in the wind tunnel: (a) two-model case, and (b) three-model case (Moriyama et al., 2010)

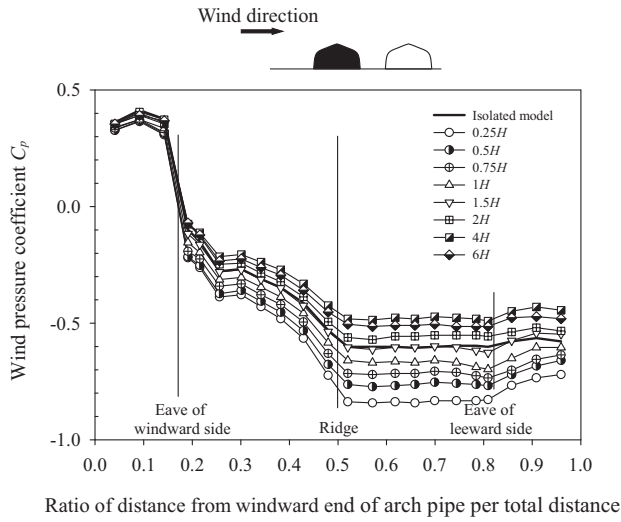


Fig. 8. C_p distribution at the central cross-section of the windward model in the two-model case (Moriyama et al., 2010)

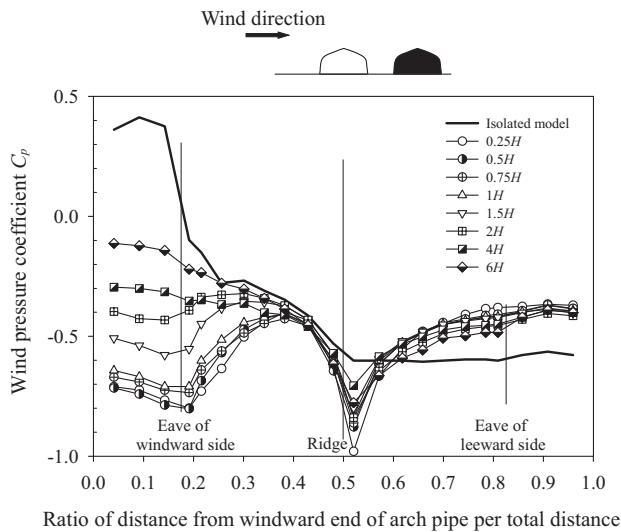


Fig. 9. C_p distribution at the central cross-section of the leeward model in the two-model case (Moriyama et al., 2010)

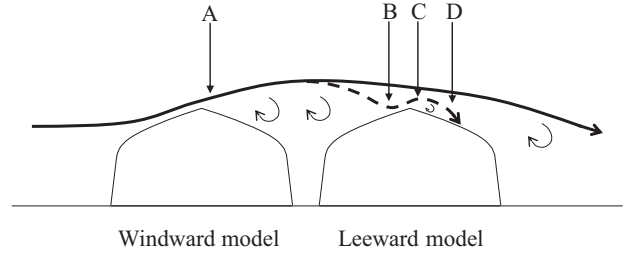


Fig. 10. Sketch of the flow pattern of separation and re-attachment on the surface of two pipe houses derived from the bubble visualization. The dotted line represents the temporary wind flow pattern, and A, B, C and D represent locations where first separation, first re-attachment, second separation, and second re-attachment occurred, respectively (Moriyama et al., 2010)

the leeward model (point C) and reattached at point D on the leeward roof of the leeward model. The curvature of the stream line between points C and D was so large that high suction were induced just behind the ridge of the leeward model.

In the three-model case, the C_p distribution on the windward side of the middle model resembled that for the leeward model in the two-model case. Conversely, the C_p value on the leeward side was generally smaller in magnitude than that for the leeward model in the two-model case.

The local lift and drag coefficients, C_L and C_D , for practical values of d_p are important for the design of pipe houses. The local lift L per unit width and drag D per ridge were computed from the C_p distribution along the central cross-section and are non-dimensional, as are the lift and drag coefficients, C_L and C_D , as follows:

$$C_L = \frac{L}{q_H S} \quad (2)$$

$$C_D = \frac{D}{q_H H} \quad (3)$$

where S is the span of pipe house, and H is the ridge height of the pipe house.

The values of C_L for the windward and second models, i.e. the leeward model in the two-model case, slightly exceeded that for the isolated model, i.e. 0.2, while the C_L value for the third model, the leeward model in the three-model case, was nearly equal to 0.2. Conversely, the C_D value significantly depended on d_p . The C_D value for the windward model exceeded that for the isolated model, i.e. 0.3; while the C_D values for the second and third models were considerably lower than 0.3. The value of C_D for the second model was negative, and the value for $d_p = 1.5H$ to $2H$ was around 0. In the practical design of pipe houses, a distance d_p of approximately $1.5H$ may be optimal to minimize drag and lift forces.

In Japan, for typical values of d_p , e.g. $d_p < 1.5H$, the observed three-dimensional effect of the gable wall on the C_p distribution is limited to a maximum distance from the gable wall of around 5 m in full scale. There may be a need to reinforce the arch pipes near the gable wall to prevent buckling.

In these studies on wind pressure, only time-averaged C_p values were discussed. However, the dynamic load effects of wind pressures have been recently considered important and were researched by Uematsu et al. (2008 and 2010) for the safe design of pipe houses.

Conclusions

Pipe houses comprise lightweight arch- and straight pipes covered with plastic film. It is a fact that most of the wind and snow damage inflicted on greenhouses affects pipe houses, hence wind and snow loads are the key external forces determining pipe house design. The main conclusions determined from the studies may be summarized as follows:

1. To investigate the economical and reasonable design of a pipe house subject to snow load, seven numerical finite element models of simple pipe house were analyzed by stress and buckling analyses, which determined the optimum bracing position for pipe houses. Adding bracing significantly increased the maximum allowable snow load for all structural size and shapes. Variation in the ridge height of the pipe house had little effect on the maximum allowable snow load during the stress analysis. However, the maximum allowable snow load determined by the buckling analysis declined with increasing ridge height, underlining the importance of the buckling analysis.
2. The wind pressure coefficients C_p on a pipe house were evaluated with a 1:20 scale model in a turbulent boundary layer. The evaluated C_p distribution for $\theta = 0^\circ$ was also

compared with specifications for greenhouses with gable and circular-arc roofs in the current design standard for greenhouse structures, and a significant difference was observed, particularly the value on the windward roof. The largest negative C_p was -3.46 near the ridge corner when $\theta = 25^\circ$. The influence of side-gable openings on the external pressure coefficient C_{pe} value was insignificant. The C_{pi} depended on the location of the openings as well as on the wind direction.

3. The C_p on the pipe houses arranged in parallel were significantly affected by the distance d_p . The C_p on the windward side of the first pipe house resembled that for an isolated pipe house, while the C_p on the roof and leeward wall were dependent on d_p . Conversely, the C_p values on the second and third pipe houses were generally negative and significantly affected by d_p . Very high suction were induced on the leeward roof of the second pipe house near the ridge. The influence of the adjacent pipe houses on the C_D was significant, while the C_L was less sensitive to d_p .

Air-inflated greenhouses, namely double-layer pipe houses, can alleviate wind pressure themselves and the effect of such alleviation is well known empirically by farmers. It is important that the behavior of such pipe houses under wind pressure be tested and discussed as future work.

Pipe houses damaged by the 2011 Earthquake and Tsunami off the Pacific Coast and by tornados on May 6, 2012 were also investigated (Moriyama et al. 2012a, Moriyama et al. 2012b). To develop techniques to reinforce pipe houses, information from these investigations should be applied to their design.

References

- Hoxey, R. P. & Richardson, G. M. (1984) Measurements of wind loads on full-scale film plastic clad greenhouses. *J. Wind Eng. Ind. Aerodyn.*, **16**, 57-83.
- Japan Greenhouse Horticulture Association (1999) *Standard for Structures of Greenhouses*. Japan Greenhouse Horticulture Association, Tokyo, Japan, pp. 152 [In Japanese].
- Mathews, E. H. & Meyer, J. P. (1987) Numerical modeling of wind loading on a film clad greenhouse. *Bldg. Environ.*, **22**, 129-134.
- Mistriotis, A. & Briassoulis, D. (2002) Numerical estimation of the internal and external aerodynamic coefficients of a tunnel greenhouse structure with openings. *Comput. Electr. in Agric.*, **34**, 191-205.
- Moriyama, H. & Toyoda, H. (1999) Characteristics of greenhouses damaged by heavy snow in January 1998 in southern Tohoku area. *Nogyo Shisetsu (J. Soc. Agric. Structures, Japan)*, **30**, 205-214 [In Japanese with English summary].
- Moriyama, H. et al. (2003a) Design consideration for small-scale pipe greenhouses to prevent arch buckling under snow load. *ASAE Annual Intl. Meeting*, Las Vegas, Nevada, USA. Paper No. 034047, 8.
- Moriyama, H. et al. (2003b) Engineering analysis of the green-

- house structures damaged by Typhoon 0221 in Chiba and Ibaraki. *Nogyo Shisetsu (J. Soc. Agric. Structures, Japan)*, **34**, 199-212 [In Japanese with English summary].
- Moriyama, H. et al. (2008a) Wind pressure coefficient of a pipe-framed greenhouse and influence of the side gable openings using a wind tunnel. *Nogyo Shisetsu (J. Soc. Agric. Structures, Japan)*, **38**, 237-248.
- Moriyama, H. et al. (2008b) Reinforcement for pipe-framed greenhouse under snow load and design optimization considering steel mass. *Nogyo Shisetsu (J. Soc. Agric. Structures, Japan)*, **38**, 263-274.
- Moriyama, H. et al. (2010) Wind tunnel study of the interaction of two or three side-by-side pipe-framed greenhouses on wind pressure coefficients. *Transactions of the ASABE*, **53**, 585-592.
- Moriyama, H. et al. (2012a) Damage of pipe-framed greenhouses by the 2011 off the Pacific coast of Tohoku earthquake tsunami. *Nogyo Shisetsu (J. Soc. Agric. Structures, Japan)*, **42**, 193-200 [In Japanese with English summary].
- Moriyama, H. et al. (2012b) Influence of three-dimensional wind direction and velocity of tornados on failure mode of pipe-framed greenhouses. *Nogyo Shisetsu (J. Soc. Agric. Structures, Japan)*, **43**, 152-159 [In Japanese with English summary].
- Ogawa, H. et al. (1989) Experimental analysis on strength of pipe-houses with ground anchoring (1) –actual size experiment-. *Nogyo Shisetsu (J. Soc. Agric. Structures, Japan)*, **19**, 29-38 [In Japanese with English summary].
- Okushima, L. & Nara, M. (1992) The tendency of greenhouse disasters. *Nogyo Shisetsu (J. Soc. Agric. Structures, Japan)*, **23**, 87-93 [In Japanese].
- Osari, H. & Yamashita, S. (1980) Studies on cross section of “pipe-house” (I). *Nogyo Kogaku Kenkyujo Giho (Tech. Rep. Natl. Res. Inst. Agric. Eng.)*, **A23**, 1-10 [In Japanese].
- Robertson, A. P. et al. (2002) Wind pressures on permeably and impermeably clad structures. *J. Wind Eng. Ind. Aerodyn.*, **90**, 461-474.
- Sase, S. et al. (1980) Ventilation of greenhouses, I. Wind tunnel measurements of pressure and discharge coefficients for a single-span greenhouse. *Nogyo Kisho (J. Agric. Meteorology)*, **36**, 3-12 [In Japanese with English summary].
- Uematsu, Y. et al. (2008) Study of wind loads on pipe-framed greenhouses -External wind pressure coefficients on enclosed structures-. *Nogyo Shisetsu (J. Soc. Agric. Structures, Japan)*, **39**, 121-132 [In Japanese with English summary].
- Uematsu, Y. et al. (2010) Peak wind pressure coefficients for designing the cladding of pipe-framed greenhouses. *Nogyo Shisetsu (J. Soc. Agric. Structures, Japan)*, **41**, 70-78 [In Japanese with English summary].